



Article scientifique

Article

2013

Published version

Open Access

This is the published version of the publication, made available in accordance with the publisher's policy.

---

## Nogo-A downregulation improves insulin secretion in mice

---

Bonal, Claire Brune; Baronnier Caffé, Delphine; Pot, Caroline; Benkhoucha, Mahdia; Schwab, Martin E; Lalive d'Epinay, Patrice; Herrera, Pedro Luis

### How to cite

BONAL, Claire Brune et al. Nogo-A downregulation improves insulin secretion in mice. In: Diabetes, 2013, vol. 62, n° 5, p. 1443–1452. doi: 10.2337/db12-0949

This publication URL: <https://archive-ouverte.unige.ch/unige:32140>

Publication DOI: [10.2337/db12-0949](https://doi.org/10.2337/db12-0949)

# Nogo-A Downregulation Improves Insulin Secretion in Mice

Claire B. Bonal,<sup>1</sup> Delphine E. Baronnier,<sup>1</sup> Caroline Pot,<sup>2,3</sup> Mahdia Benkhoucha,<sup>2</sup> Martin E. Schwab,<sup>4,5</sup> Patrice H. Lalive,<sup>2,3,6</sup> and Pedro L. Herrera<sup>1</sup>

Type 2 diabetes (T2D) is characterized by  $\beta$ -cell dysfunction and the subsequent depletion of insulin production, usually in a context of increased peripheral insulin resistance. T2D patients are routinely treated with oral antidiabetic agents such as sulfonylureas or dipeptidyl peptidase-4 antagonists, which promote glucose- and incretin-dependent insulin secretion, respectively. Interestingly, insulin secretion may also be induced by neural stimulation. Here we report the expression of Nogo-A in  $\beta$ -cells. Nogo-A is a membrane protein that inhibits neurite outgrowth and cell migration in the central nervous system. We observed that Nogo-A-deficient mice display improved insulin secretion and glucose clearance. This was associated with a stronger parasympathetic input and higher sensitivity of  $\beta$ -cells to the cholinergic analog carbachol. Insulin secretion was also improved in diabetic *db/db* mice treated with neutralizing antibody against Nogo-A. Together, these findings suggest that promoting the vagal stimulation of insulin secretion through the selective inhibition of Nogo-A could be a novel therapeutic approach in T2D. *Diabetes* 62:1443–1452, 2013

**T**he relative or absolute lack of insulin is responsible for diabetes. In type 1 diabetes,  $\beta$ -cell loss is due in most cases to an autoimmune reaction, but not exclusively (1). In type 2 diabetes (T2D), increased peripheral insulin resistance challenges the functional  $\beta$ -cell mass; after an initial attempt at overriding the increased insulin demand, the number of cells that produce insulin declines progressively.

Glucose entry into cells is regulated by insulin, whose secretion from  $\beta$ -cells is tightly coordinated by different secretagogues. Insulin secretion is initiated by the cholinergic parasympathetic stimulation of  $\beta$ -cells (the so-called “cephalic phase”) and subsequently potentiated during the enteric “absorptive phase” (2). In response to mechanical and chemical stimulation along the digestive tract, the intestinal incretin hormones glucagon-like peptide-1 (GLP-1) and gastric inhibitory peptide (GIP) potentiate insulin secretion directly and indirectly, through neuronal stimulation (the “incretin effect”) (3–5). Progressively, nutrient

absorption and increased blood glucose stimulate insulin secretion directly (post-absorptive phase) (6). Altogether, different secretagogues act synergistically and trigger the adequate biphasic release of insulin from  $\beta$ -cells, primed by cholinergic stimulation (7). These secretagogues reach islet endocrine cells through the vascular and neural networks. Pancreas innervation consists of parasympathetic (vagus nerve) and sympathetic efferent fibers and afferent sensory fibers (splanchnic nerve), and of intrapancreatic parasympathetic ganglion cells. The vagal input stimulates the secretion of insulin and other islet hormones, such as pancreatic polypeptide (PP) via cholinergic (i.e., mediated by acetylcholine) and noncholinergic mechanisms (8–10). Sympathetic postganglionic terminal nerves release nor-adrenaline or other peptides on endocrine cells; this represses insulin and somatostatin secretion while promoting glucagon release (11). The afferent sensory fibers innervate the periphery of islets and release calcitonin gene-related peptide (CGRP), among other peptides (12,13).

$\beta$ -Cells and neurons share numerous features. They are electrically excitable, release mediators in response to membrane depolarization, and extend neurite-like processes (14). In addition,  $\beta$ -cells express many neuronal proteins (14,15), such as the neurotransmitter  $\gamma$ -aminobutyric acid (GABA) (16,17) or the synaptic cell-surface molecules neurexin, neuroligin, and SynCAM (18,19). Among them, neurexin and neuroligin have been shown to participate in insulin secretion (18,19).

Nogo-A is a high-molecular-weight membrane protein mostly expressed in the central nervous system (CNS), oligodendrocytes, and subsets of neurons (20,21), as well as other tissues, such as skeletal muscle (22). Nogo-A restricts neuronal regeneration in injured adult spinal cord and brain and limits plastic rearrangements and functional recovery after large CNS lesions, such as after spinal cord dorsal hemisection (23–25). In the intact CNS, Nogo-A appears to have a stabilizing and controlling role in axonal sprouting and cell migration (26–28). Cytoskeletal regulators, such as Rho GTPases or cofilin, mediate the axonal and neurite growth inhibitory action of Nogo-A (28,29). Nogo-A and its receptor (NgR) are also found in synapses, where they may influence their stability and function (30–32).

Here we show that Nogo-A is expressed in pancreatic islets. We thus explored its potential role on endocrine pancreas function using mice lacking the two active Nogo-A alleles (33,34), which were challenged with different insulin secretagogues. Compared with wild-type animals, Nogo-A knockout (KO) mice presented increased insulin secretion, resulting in higher glucose clearance. This enhanced insulin release resulted from a higher pancreatic parasympathetic input on islets and from a higher sensitivity of  $\beta$ -cells to cholinergic and GLP-1 stimulation. We

From the <sup>1</sup>Department of Genetic Medicine and Development, Faculty of Medicine, University of Geneva, Geneva, Switzerland; the <sup>2</sup>Division of Neurology, Department of Neurosciences, Geneva University Hospital, Geneva, Switzerland; the <sup>3</sup>Department of Pathology and Immunology, Faculty of Medicine, University of Geneva, Geneva, Switzerland; the <sup>4</sup>Brain Research Institute, University of Zurich, Zurich, Switzerland; the <sup>5</sup>Department of Biology, Swiss Federal Institute of Technology, Zurich, Switzerland; and the <sup>6</sup>Division of Laboratory Medicine, Department of Genetic and Laboratory Medicine, Geneva University Hospital, Geneva, Switzerland.

Corresponding author: Pedro L. Herrera, pedro.herrera@unige.ch.

Received 17 July 2012 and accepted 17 November 2012.

DOI: 10.2337/db12-0949

This article contains Supplementary Data online at <http://diabetes.diabetesjournals.org/lookup/suppl/doi:10.2337/db12-0949/-/DC1>.

© 2013 by the American Diabetes Association. Readers may use this article as long as the work is properly cited, the use is educational and not for profit, and the work is not altered. See <http://creativecommons.org/licenses/by-nc-nd/3.0/> for details.

obtained similar results, i.e., improved insulin secretion associated with a higher responsiveness of  $\beta$ -cells, in diabetic *db/db* mice treated for a short period with neutralizing antibody against Nogo-A. Together, these observations reveal that Nogo-A is implicated in pancreatic endocrine function and thence in the control of glucose homeostasis.

## RESEARCH DESIGN AND METHODS

**Mice.** *Nogo-A*<sup>-/-</sup> KO mice were described previously by one of us (33). In all experiments, C57BL/6J Nogo-A KO male mice were compared with age-matched C57BL/6J wild-type males. Genotyping was performed by PCR from genomic DNA isolated from tail biopsies using M58 (TGCTTTGAATTATTC-CAAGTAGTCC) and M101 (AGTGAGTACCAGCTGCAC) primers for wild-type Nogo-A allele (1.4-kb band), and M58 and M63 (CCTACCCGGTAGAA-TATCGATAAGC) primers for the Nogo-A-deleted allele (1.2-kb band). Five-week-old male *db/db* homozygous mice (C57BL/Ks background; BKS. Cg-Dock7 m<sup>+/+</sup> Lep<sup>db</sup>/J strain) were purchased from Charles River Laboratories (L'Arbresle, France), for the treatment with neutralizing anti-Nogo-A 11C7 mouse antibody (25). *Pdx1-GFP* (35) and *RIP-DTR* (36) mice were previously described. Animals were maintained in a temperature-controlled room, on a 12-h light-dark cycle, and fed standard rodent chow ad libitum. The Direction Générale de la Santé of the Canton de Genève approved the study.

**Islet isolation.** Mice were killed and their pancreata exposed. After clamping at the porta hepatis (transverse fissure of the liver), the main pancreatic duct was cannulated with a 27-gauge butterfly needle and retrogradually injected with 2 mL of collagenase XI (2 mg/mL in Hanks' balanced salt solution) (Sigma-Aldrich). After dissection, the pancreas was digested in 3 mL of collagenase XI solution for 15 min at 37°C and finally disrupted upon vigorous shaking. Islets were then purified on a Histopaque 1119 (Sigma-Aldrich) gradient, washed three times with Hanks' 1× BSA 0.1%, and finally "fished" (i.e., handpicked) twice to increase purity.

**Fluorescence-activated cell sorter analysis.** For fluorescence-activated cell sorter (FACS) sorting of GFP<sup>+</sup> cells, isolated *Pdx1-GFP* islets were dissociated into a single-cell suspension with trypsin 0.25%. Live  $\beta$ -cells were isolated as DAPI-GFP<sup>+</sup> cells by FACS with MoFlo (Dako-Cytomation).

**RT-PCR.** Total RNA from the brain (cerebrum), sciatic nerve, pancreas, and isolated islets of C57BL/6J control mice were extracted with the RNeasy mini kit (Qiagen) and RNeasy micro kit (Qiagen), respectively. Total RNA from sorted  $\beta$ -cells was extracted using Trizol. cDNA were prepared using Superscript II RT kit (Invitrogen), and thereafter PCR was performed with the Red Taq kit (Sigma-Aldrich). The 5' and 3' primers were chosen from different exons. The sequences of the primers are available upon request.

**Western blotting.** Brain, sciatic nerves, pancreas, and isolated islets from Nogo-A KO and C57BL/6J mice were homogenized using a polytron in lysis buffer (50 mmol/L Tris-HCl, pH 7.5, 250 mmol/L NaCl, 1% Triton X-100, 1 mmol/L EDTA, and 1 mmol/L dithiothreitol) containing complete protease inhibitors (Roche) and incubated for 30 min on ice. Lysates were sonicated and clarified by centrifugation. Protein concentrations were then determined. Whole cell extract samples were fractionated by SDS-PAGE and transferred to Immobilon-P membranes (Millipore) for immunoblotting with anti-Nogo-A 11C7 (1/10,000; M.E.S.) and rabbit anti- $\beta$ -actin antibody (1/5,000). Detection was performed using peroxidase-conjugated anti-rabbit IgGs (1/5,000; Promega). Bands were visualized by enhanced chemiluminescence (ECL; Amersham) according to the manufacturer's instructions.

**Immunofluorescence and immunohistochemistry.** Collected pancreata were weighted and then rinsed in cold PBS and fixed overnight at 4°C in paraformaldehyde 4%. Tissues were dehydrated, embedded in paraffin, and sectioned at 5  $\mu$ m with a microtome. The primary antibodies used for immunofluorescence were mouse antiglucagon (1/1,000; Sigma-Aldrich), guinea pig anti-insulin (1/400; Dako), rabbit anti-PP (1/200; Bachem), rabbit anti-somatostatin (1/200; Dako), rabbit anti-Pdx1 (1/5,000; gift from Chris Wright, Vanderbilt University, Nashville, TN), rabbit anti-MafA (1/500; Bethyl Laboratory), rabbit anti-Nkx6.1 (1/800; ICBBC), rabbit anti-Glut-2 (1/200; gift from Bernard Thorens, Center for Integrative Genomics, University of Lausanne, Switzerland), and rabbit anti-PC1/3 (1/200; gift from Ole Madsen, Novo Nordisk, Bagsvaerd, Denmark).

For immunohistochemistry, dewaxed and rehydrated sections were permeabilized in 0.1% Triton X-100, washed, and blocked in 3% BSA and 0.1% Tween in PBS. The primary antibodies were incubated overnight. After washing in PBS, sections were incubated with specific secondary antibodies coupled to either Alexa 488 (Molecular Probes) or Cy3 (Jackson ImmunoResearch). Both islet cell mass and  $\beta$ -cell mass were assessed by measuring the endocrine synaptophysin-positive area, or the insulin-positive area, on four different sections, separated by 200  $\mu$ m each ( $n = 3$ ), multiplied by the pancreas weight.

Specimens were mounted in polyvinyl alcohol and examined with a Leica confocal microscope (DM 5500). Tissue surface and cell numbers were measured with NIH Image J 1.60 or Bitplane Imaris (v7.0) softwares.

**In vivo insulin secretion assays.** For intraperitoneal glucose tolerance tests (ipGTTs), overnight-fasted animals ( $n = 10$ ) received an intraperitoneal glucose injection (2 g/kg) (Sigma-Aldrich), and blood was collected from the tail vein at 0, 15, 30, 60, 90, and 120 min into centrifuge tubes treated with lithium heparin. For intravenous GTTs, overnight-fasted animals ( $n = 7$ ) were anesthetized with isoflurane and injected with a solution of glucose alone (1 g/kg) or supplemented with 0.53  $\mu$ mol/L carbachol (Sigma-Aldrich) (37) into the retroorbital capillary plexus. Blood samples were collected from the retro-orbital plexus at 0, 1, 5, 20, and 50 min into centrifuge tubes treated with lithium heparin. Blood glucose was assessed with Glucometer Dex2 (Bayer Corporation). Glycemic area under the curve was measured from time 0 to 120 min, after subtraction of basal glycemia. After immediate centrifugation, plasma was separated and insulin levels assessed with the Ultrasensitive Rat Insulin ELISA kit (Mercodia).

**Insulin tolerance tests.** Animals fasted for 6 h were intraperitoneally injected with recombinant human insulin (0.5 units/kg, Actrapid; Novo Nordisk), and blood glucose was measured from the tail vein at 15, 30, 45, 60, and 120 min.

**Protein extraction and hormone content measurements.** Pancreata collected for hormone measurements were homogenized in 5 mL ( $n = 5$ –11) acid-ethanol solution (74% ethanol and 1.4% HCl). Samples were sonicated and centrifuged. The supernatants were submitted to immunoassay experiments using either the Glucagon RIA kit (Linco) or Ultrasensitive Rat Insulin ELISA kit for glucagon and insulin content measurements, respectively.

**In vitro insulin secretion assays.** Batches of 10 isolated islets from four mice were preincubated for 30 min in 1 mL Krebs-Ringer bicarbonate HEPES buffer (KRBH) supplemented with 0.1% BSA and 1.4 mmol/L glucose at 37°C. Next, the supernatant was replaced by 0.5 mL KRBH supplemented with 0.1% BSA and 1.4, 2.8, 4.2, 8.4, and 16.8 mmol/L glucose was added for another 30 min at 37°C ( $n = 3$ –4). Additionally, islets were incubated for 30 min in 0.5 mL KRBH containing glucose, 0.1% BSA, and 10  $\mu$ mol/L carbachol (Sigma-Aldrich) or 100 nmol/L GLP-1 (Bachem) ( $n = 3$ –4) (38,39). Secreted and total insulin in the supernatant was measured in micrograms per liter with the Ultrasensitive Rat Insulin ELISA kit. Similar insulin contents between islet batches were assessed after removal of the supernatant and acid-ethanol extraction. Secreted insulin was reported as the percentage of secreted insulin normalized to the total insulin content of 10 islets.

**Vagal stimulation of islet hormone secretion.** 2-Deoxy-D-glucose (2DG) (Sigma-Aldrich) was injected intravenously (50 mg/kg) into 2-month-old adult control and Nogo-A KO mice ( $n = 5$ ). For PP, mice were fasted overnight and blood samples were collected at 0, 15, and 30 min (40). For GLP-1 and GIP, mice were kept with access to food, and blood samples were collected at 0 and 10 min (40). Blood samples were collected from the retrobulbar capillary plexus of anesthetized mice in chilled tubes treated with lithium-heparin. For plasma GLP-1 and GIP measurements, according to the manufacturer's protocol, dipeptidyl peptidase-4 inhibitor (Millipore) was added in tubes and blood samples were immediately processed. Plasma was assayed for total GIP, GLP-1, and PP using a MILLIPLEX mouse gut hormone kit (#MGT-78 K; Millipore) and the Bioplex (Bio-Rad) at the Mouse Metabolic Evaluation Facility (Center for Integrative Genomics, University of Lausanne, Lausanne, Switzerland).

**In vivo administration of neutralizing anti-Nogo-A 11C7 antibody.** Neutralizing anti-Nogo-A 11C7 mouse antibody (Novartis) and nonspecific anti-BrdU mouse antibody (AbSerotec) were intravenously infused once a week (2,450 ng/dose), during 2 weeks (4,900 ng in total) through the retro-orbital capillary plexus in anesthetized mice.

**Statistical analysis.** All results were reported as mean  $\pm$  SEM. Groups were compared with nonparametric tests (one tailed Mann-Whitney), reported as *P* values. All tests were performed using the GraphPad Prism software.

## RESULTS

**Nogo-A is expressed in endocrine cells of the pancreas.** In the adult mouse pancreas (2-month-old males), we detected by RT-PCR the expression of *Rtn4a* (Nogo-A transcript) in extracts from isolated islets of Langerhans (Fig. 1A). *Rtn4a* transcripts were also found in EGFP<sup>+</sup>  $\beta$ -cells isolated by flow cytometry [obtained from *Pdx1-EGFP* transgenic mice (35)] (Fig. 1A). *Rtn4a* expression in  $\beta$ -cells was confirmed by deep sequence analysis performed on RNA extracts of  $\beta$ -cell-depleted islets obtained from *RIP-DTR* transgenic mice treated with diphtheria toxin (36) (Supplementary Fig. 1A). Finally, islet expression of Nogo-A at the protein level was observed

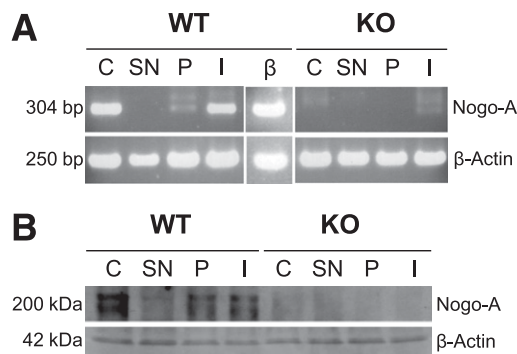


**FIG. 1.** Nogo-A is expressed in endocrine and neuronal compartments of the pancreas. **A:** Expression of Nogo-A in the brain (cerebrum, C), sciatic nerve (SN), pancreas (P), islets (I), and sorted  $\beta$ -cells ( $\beta$ ) in 2-month-old controls and Nogo-A KO mice, as assessed by RT-PCR.  $\beta$ -actin is used as internal control. **B:** Expression of Nogo-A in the brain (C), sciatic nerve (SN), pancreas (P), and islets (I) in 2-month-old wild-type and Nogo-A KO mice, as assessed by Western blotting.  $\beta$ -Actin is used as internal control.

by Western blot (Fig. 1B). We observed *Rtn4a* transcripts in human and rat islets as well (Supplementary Fig. 1B). **Nogo-A KO mice display increased insulin secretion and lower glycemia, yet they have a normal  $\beta$ -cell mass.** The pancreatic expression of Nogo-A led us to wonder whether Nogo-A regulates insulin secretion, like neurotrophin (18). Body weight as well as the pancreas-to-body weight ratio was unchanged in Nogo-A KO mice (body weight: wild type  $28.47 \pm 0.86$  g, KO  $23.82 \pm 1.89$  g;  $n = 10$ ,  $P = \text{NS}$ ; pancreas-to-body weight ratio: wild-type  $0.99 \pm 0.05\%$ , KO  $0.86 \pm 0.09\%$ ;  $n = 5$ ,  $P = \text{NS}$ ) (Fig. 2A and B). We measured plasma values of glucose, insulin, and glucagon in fasted and random-fed conditions. After 16-h fasting, plasma glucose, insulin, and glucagon levels were normal in KO mice (Fig. 2C–E). However, in a random-fed situation (a period during which insulin secretion is stimulated by glucose, glucocorticoids, and neurotransmitters), KO animals had significantly less blood glucose (wild type  $10.66 \pm 0.35$  mmol/L, KO  $8.48 \pm 0.31$  mmol/L;  $n = 5$ ,  $P = 0.04$ ), associated with increased insulinemia (wild type  $0.50 \pm 0.02$   $\mu\text{g/L}$ , KO  $1.23 \pm 0.28$   $\mu\text{g/L}$ ;  $n = 6$ ,  $P = 0.04$ ) (Fig. 2C and D), but normal glucagonemia (wild type  $60.79 \pm 4.62$  pg/L, KO  $66.54 \pm 13.29$  pg/L;  $n = 6$ ,  $P = \text{NS}$ ) (Fig. 2C–E).

At the histological level, islet number, structure, size, and shape and  $\beta$ -cell mass were normal in Nogo-A KO mice (Supplementary Fig. 2A–E and not shown). The total pancreatic glucagon content was unchanged (wild type  $338.07 \pm 8.92$  pg, KO  $344.02 \pm 4.96$  pg;  $n = 9$ –11,  $P = \text{NS}$ ) (Supplementary Fig. 2G), and the pancreatic insulin content was slightly increased (wild type  $554.65 \pm 54.54$  ng, KO  $763.51 \pm 37.67$  ng;  $n = 5$ ,  $P < 0.05$ ), thus suggesting that insulin content per  $\beta$ -cell was somewhat augmented (Supplementary Fig. 2F).

These observations reveal that although Nogo-A KO mice have a normal  $\beta$ -cell mass, they exhibit lower glycemia associated with higher insulin secretion in the random-fed condition, but without overt hypoglycemia.

**Cholinergic-dependent glucose-stimulated insulin secretion is enhanced in Nogo-A KO mice.** In order to study the enhanced insulin secretion, we performed GTTs in response to different secretagogues (glucose alone or supplemented with carbachol) and after different routes of administration (intraperitoneal or intravenous injection).

Besides increased plasma glucose and cholinergic stimulation (carbachol), insulin secretion from  $\beta$ -cells is also induced in response to the stimulated parasympathetic nervous system upon intraperitoneal injection of glucose (41). Overnight-fasted Nogo-A KO animals showed improved glucose clearance after intraperitoneal glucose administration (2 g/kg), as revealed by a decreased area under the curve (wild type  $709.875 \pm 72.73$  mmol/L/min, KO  $378.95 \pm 31.17$  mmol/L/min;  $n = 4$ ,  $P = 0.01$ ) (Fig. 3A). The stimulated insulin secretion was significantly higher 1 h after glucose injection in Nogo-A KO animals (Fig. 3B). Since insulin sensitivity was comparable in KO and wild-type mice (Fig. 3C), the faster glucose clearance in the former was thus due to a higher insulin secretion. We then explored the means by which insulin secretion is potentiated in Nogo-A KO mice. Therefore, after overnight fasting, animals were exposed to an intravenous bolus of either glucose alone (1 g/kg) (Fig. 3D and E) or glucose supplemented with the cholinergic analog carbachol ( $0.53$   $\mu\text{mol/L}$ ), so as to mimic the vagal stimulation (Fig. 3F and G). Although control and KO mice similarly corrected the induced hyperglycemia by secreting comparable amounts of insulin in response to glucose (Fig. 3D–E), insulin secretion was higher in the KO group when animals were treated additionally with carbachol (Fig. 3F and G). Taken together, these observations suggest that in the absence of Nogo-A activity, the cholinergic vagal stimulation on  $\beta$ -cells triggers a stronger release of insulin.

**The increased insulin secretion in Nogo-A KO mice is associated with higher parasympathetic input on islet cells.** We reasoned that the enhanced insulin secretion in Nogo-A KO mice might rely upon higher islet parasympathetic input or increased  $\beta$ -cell responsiveness, or both. The density of parasympathetic (VACHT<sup>+</sup>), sympathetic (VMAT2<sup>+</sup>), and sensory (CGRP<sup>+</sup>) fibers was normal in Nogo-A KO pancreas (not shown). We assessed the vagal stimulation on  $\beta$ -cells through the administration of 2DG (50 mg/kg; intravenously). 2DG is an unmetabolizable glucose analog that blocks intracellular glucose utilization, thus inducing neuroglycopenia and subsequently stimulating the vagus nerve, which promotes islet hormone secretion (12,42). We estimated the parasympathetic input on islets by measuring the fasting plasma PP, whose secretion is strictly controlled by parasympathetic stimulus (43,44). Whereas plasma PP was identical in the two groups of mice before 2DG injection, 30 min after 2DG, this value was almost doubled in Nogo-A KO mice (wild type  $101.08 \pm 11.45$  pg/mL, KO  $187.09 \pm 15.33$  pg/mL;  $n = 4$ ,  $P < 0.05$ ), suggesting an increased parasympathetic input (Fig. 4A). In parallel, we measured the postprandial plasma glucocorticoids, before and after 2DG injection. GLP-1 was undetectable, as previously reported (45), yet we could determine that plasma GIP values were lower in Nogo-A KO mice, irrespective of 2DG treatment, which correlates with their lower glycemia (Fig. 2C) (before 2DG: wild type  $58.05 \pm 4.90$  pg/mL, KO  $34.86 \pm 3.03$  pg/mL,  $P < 0.005$ ; 15 min after 2DG: wild type  $51.90 \pm 4.65$  pg/mL, KO  $36.55 \pm 4.19$  pg/mL,  $P < 0.05$ ,  $n = 5$ ) (Fig. 4B). Combined, the above observations corroborate that the vagal stimulation of insulin secretion is reinforced by a higher parasympathetic tone in Nogo-A KO mice.

Using isolated islets, we assessed the responsiveness of  $\beta$ -cells to various secretagogues downstream of the parasympathetic stimulation. Groups of 10 islets with similar insulin content from control and Nogo-A KO mice responded similarly to various concentrations of glucose

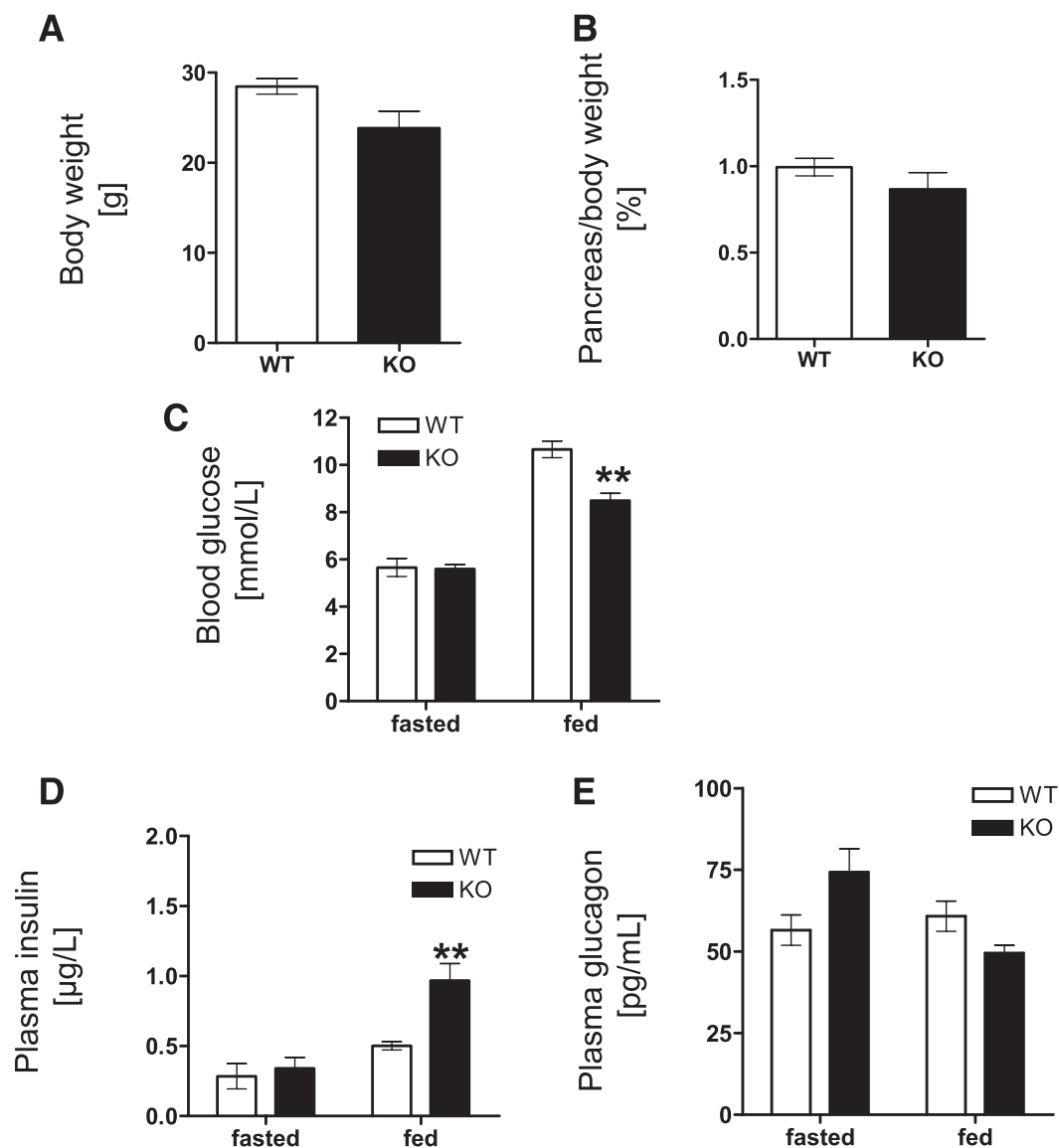


**FIG. 2.** Nogo-A KO mice have high plasma insulin in the random-fed condition. Body weight ( $n = 10$  mice,  $P = \text{NS}$ ) (A) and the relative pancreatic weight ( $n = 5$ ,  $P = \text{NS}$ ) (B) remain unaffected in Nogo-A KO mice. C: Blood glucose is significantly decreased in the random-fed condition in KO animals, as compared with wild type ( $n = 5-6$ ,  $P < 0.05$ ). D: Plasma insulin in the random-fed condition is higher in KO mice ( $n = 5-6$ ,  $P < 0.05$ ). E: Plasma glucagon remains constant in wild-type and KO animals, whether in fasted or random-fed conditions ( $n = 5-6$ ,  $P = \text{NS}$ ). \*\* $P < 0.005$ .

(Fig. 4C). Accordingly, the expression of  $\beta$ -cell machinery genes (*Insulin1*, *Insulin2*, *Slc2a2*, *GK*, *MafA*, *Nkx6.1*, *Pdx1*, *NeuroD1*, *Kcnj11*, *PC1*, *Gpr35*, *Htr7*, *Slc24a*, and *Trpm2*) was fundamentally not altered, even though one gene, *Trpm2*, a regulator of insulin secretion (46), was upregulated in Nogo-A KO animals (Supplementary Fig. 3). Islets were then submitted to different glucose concentrations, supplemented with carbachol (CC; 100  $\mu\text{mol/L}$ ). In this situation, insulin secretion was increased in Nogo-A KO islets, as compared with control islets (1.4 mmol/L + CC: wild type  $0.070 \pm 0.008\%$ , KO  $0.195 \pm 0.025\%$ ,  $P < 0.005$ ; 8.4 mmol/L + CC: wild type  $0.170 \pm 0.025\%$ , KO  $0.287 \pm 0.036\%$ ,  $n = 7-13$ ,  $P < 0.05$ ) (Fig. 4D). Finally, islets were incubated with glucose (8.4 mmol/L) supplemented with GLP-1 (100 nmol/L). Insulin secretion in response to glucose + GLP-1 was similar between wild-type and KO islets (Fig. 4E). These observations reveal that isolated Nogo-A KO islets secrete more insulin specifically in response to glucose supplemented with carbachol.

**Diabetic *db/db* mice display improved insulin secretion after administration of neutralizing anti-Nogo-A antibody.** The constitutive inactivation of Nogo-A confers to metabolically healthy mice the ability to more efficiently correct the induced hyperglycemia thanks to an improved insulin secretion. In order to explore the relevance of these observations to diabetes, we investigated the capacity of neutralizing anti-Nogo-A monoclonal antibody (termed 11C7) to promote insulin secretion in recent-onset T2D animals. Five-week-old diabetic *db/db* mice (i.e., lacking the leptin receptor) were treated with either anti-Nogo-A or control (anti-BrdU) antibody, as previously described (23). 11C7 was previously reported to inhibit Nogo-A in the CNS of adult rats, where it enhances the sprouting and regrowth of injured spinal cord axons (23). In brief, mice received two intravenous injections of 4.9 mg antibody (245 mg/kg), either 11C7 or control antibody, during a 2-week period. One week after the second injection, insulinemia in random-fed *db/db* mice treated

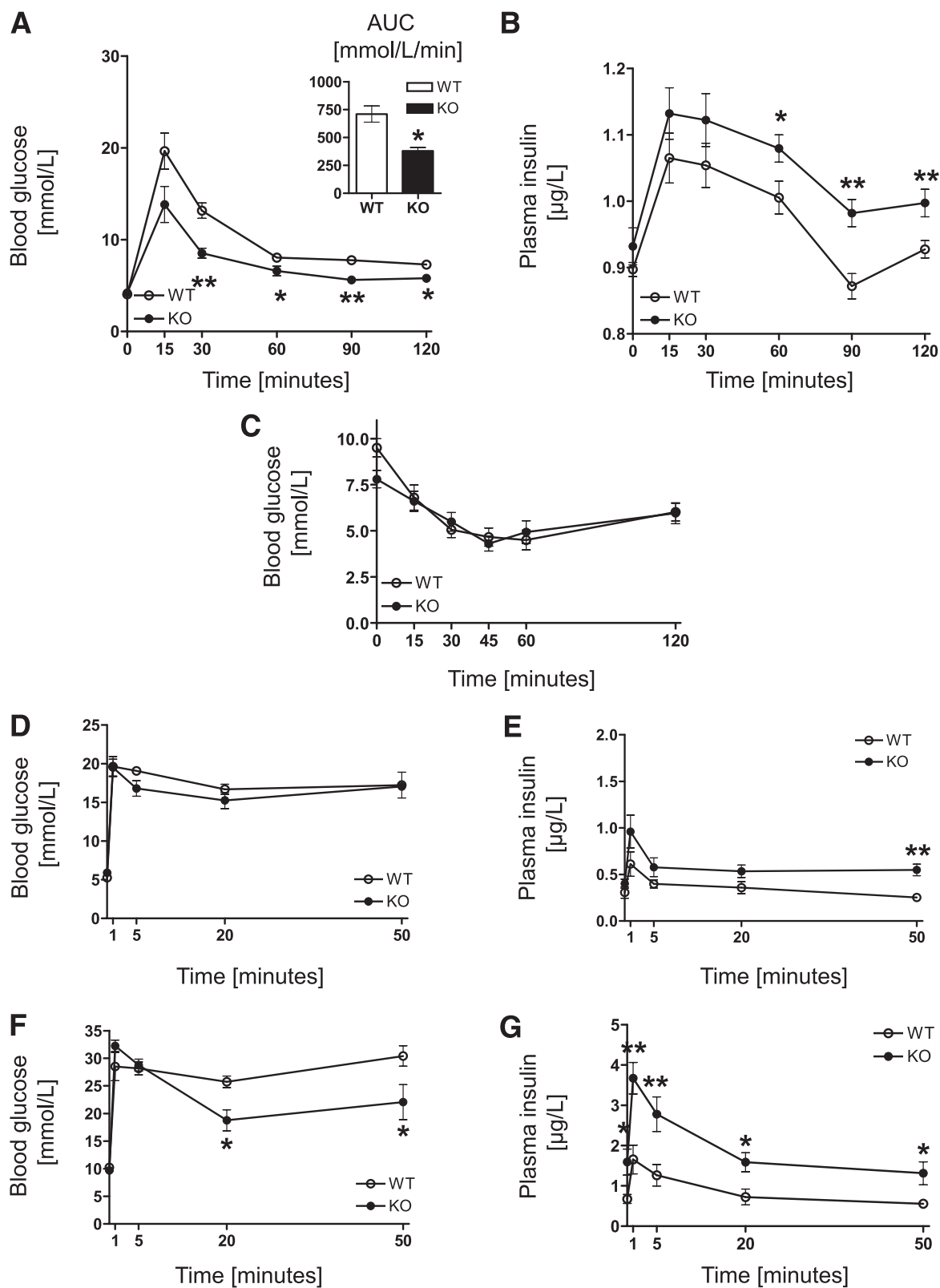


**FIG. 3.** Improved insulin secretion in Nogo-A KO mice in response to simultaneous glucose and nervous stimulation. **A:** Blood glucose (mmol/L) after intraperitoneal injection of 2 g/kg glucose is cleared faster in KO mice than in controls ( $n = 5$ ,  $*P < 0.05$ ,  $**P < 0.005$ ). **B:** Plasma insulin ( $\mu$ g/L) during ipGTTs is higher ( $n = 10$ ,  $*P < 0.05$ ,  $**P < 0.005$ ). **C:** Blood glucose after intraperitoneal injection of 0.5 units/kg insulin is similar between wild type and KO ( $n = 7-8$ ,  $P = \text{NS}$ ). Blood glucose (**D**) and plasma insulin (**E**) after intravenous injection of glucose (1 g/kg). Both wild-type and KO groups have a broadly similar glucose clearance and insulin level ( $n = 5-6$ ,  $P = \text{NS}$ ). Blood glucose (**F**) and plasma insulin (**G**) after intravenous injection of glucose (1 g/kg) supplemented with the cholinergic analog carbachol ( $0.53 \mu\text{mol/L}$ ). Compared with controls, KO mice present an improved glucose clearance, associated with a more potent insulin secretion ( $n = 5-6$ ,  $*P < 0.05$ ,  $**P < 0.005$ ).



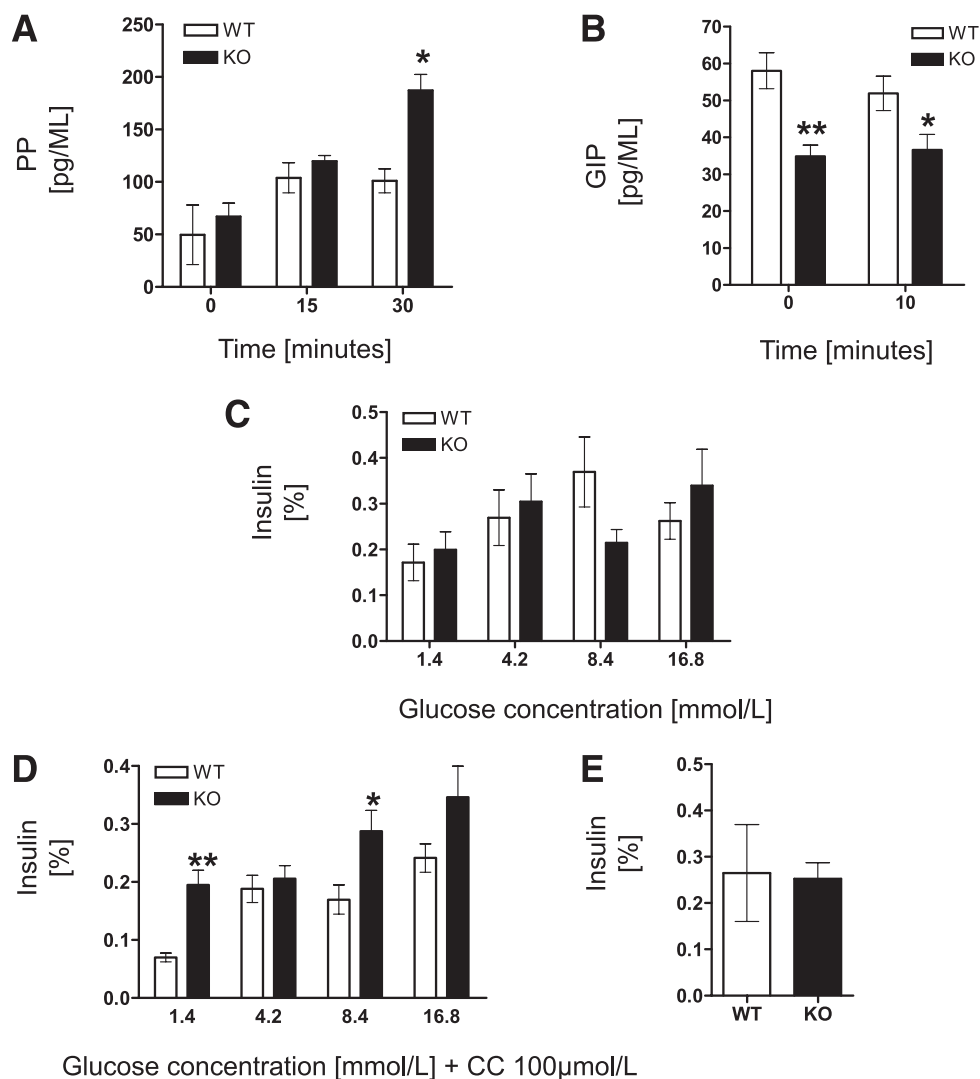


**FIG. 4.** Nogo-A KO mice have a higher parasymphetic tone, and their  $\beta$ -cells are more sensitive to glucose supplemented with carbachol. **A:** After intravenous injection of 50 mg/kg 2DG, which triggers neuroglycopenia and a subsequent parasymphetic stimulation, plasma PP levels (pg/mL) in overnight-fasted Nogo-A KO mice are higher than in controls ( $n = 5$ ,  $*P < 0.05$ ,  $**P < 0.008$ ). **B:** Plasma GIP (pg/mL) in random-fed Nogo-A KO mice is lower than in controls ( $n = 5$ ,  $*P < 0.05$ ,  $**P < 0.008$ ). **C–E:** Sensitivity of  $\beta$ -cells from isolated wild-type and Nogo-A KO islets. **C:** In response to glucose only, wild-type and Nogo-A KO islets secrete insulin similarly ( $n = 16$  batches of 10 islets from four mice,  $P = \text{NS}$ ). **D:** In response to glucose supplemented with carbachol (CC; 100  $\mu\text{mol/L}$ ), Nogo-A KO isolated islets secrete significantly more insulin than wild-type islets ( $n = 15$  batches of 10 islets, four mice,  $*P < 0.05$ ,  $**P < 0.005$ ). **E:** In response to 8.4 mmol/L glucose supplemented with GLP-1 (100 nmol/L), KO isolated islets secrete similar insulin as wild-type islets ( $n = 15$  batches of 10 islets, three mice,  $P = \text{NS}$ ).

with anti-Nogo-A antibody was higher than in control antibody-treated animals (control  $13.94 \pm 5.02 \mu\text{g/L}$ , 11C7  $32.28 \pm 8.14 \mu\text{g/L}$ ;  $n = 3$ ,  $P < 0.05$ ), yet the total pancreatic insulin content remained unchanged (not shown). No effect was detected on glucose levels or body weight, most probably due to the described severe insulin resistance in peripheral tissues in *db/db* mice, and also perhaps to the shortness of the treatment period. Antibody-treated *db/db* mice underwent different metabolic challenges, as follows. During ipGTTs, *db/db* mice treated with anti-Nogo-A had higher plasma insulin (15-min control  $1.25 \pm 0.08 \mu\text{g/L}$ , 11C7  $2.17 \pm 0.15 \mu\text{g/L}$ ;  $n = 3$ –4,  $P < 0.05$ ) (Fig. 5A). In another experiment, we assessed the glucose-induced insulin secretion by intravenously providing a bolus of glucose (1 g/kg); in this situation, plasma insulin levels were similar most of the time in anti-Nogo-A-treated mice, like in Nogo-A KO mice (Fig. 2E and Fig. 5B). Yet when the mice were given glucose and carbachol (0.53  $\mu\text{mol/L}$ )

simultaneously, insulin secretion was fourfold higher on average in anti-Nogo-A-treated *db/db* animals (control  $10.65 \pm 2.14$ , 11C7  $46.43 \pm 8.00$ ;  $n = 3$ ,  $P < 0.05$ ) (Fig. 5C) while the total pancreatic insulin content remained steady (not shown).

We reasoned that the higher insulin secretion observed in *db/db* mice treated with anti-Nogo-A neutralizing antibody could result from a higher parasymphetic input and/or from higher  $\beta$ -cell cholinergic sensitivity, as in Nogo-A KO mice. We therefore indirectly assessed the parasymphetic tone after 2DG-induced neuroglycopenia by measuring the plasma levels of PP, as above. Interestingly, fasting basal PP levels before 2DG stimulation are comparable between healthy wild-type animals and control *db/db* mice (not shown), yet after 2DG injection, they become twofold higher in control *db/db* animals (wild type  $101.08 \pm 11.45 \text{ pg/mL}$ , control *db/db*  $252.78 \pm 46.56 \text{ pg/mL}$ ). In anti-Nogo-A-treated *db/db* mice, 2DG injection

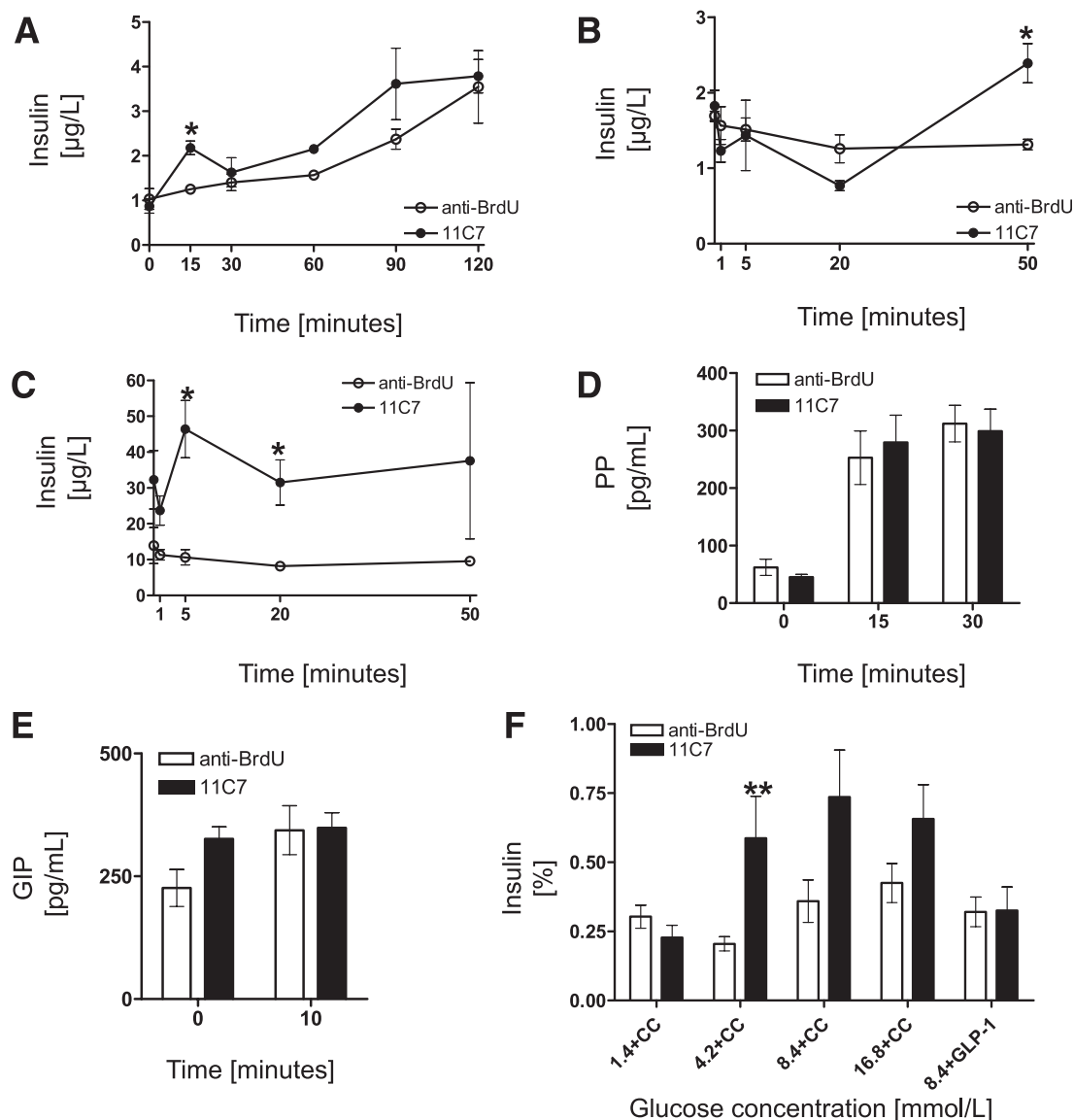


**FIG. 5.** Insulin secretion is improved in diabetic *db/db* mice treated with anti-Nogo-A neutralizing antibody (11C7). **A–C:** Plasma insulin levels ( $\mu\text{g/L}$ ) after injection of glucose are higher in mice treated with anti-Nogo-A antibody than in controls. **A:** Intraperitoneal injection of 2 g/kg glucose ( $n = 2-4$ ,  $*P < 0.05$ ). **B:** Intravenous injection of glucose (1 g/kg) ( $n = 3$ ,  $*P < 0.05$ ). **C:** Intravenous injection of glucose (1 g/kg) supplemented with carbachol (CC; 0.53  $\mu\text{mol/L}$ ), which triggers the parasympathetic stimulation. **D:** The plasma PP levels (pg/mL) in anti-Nogo-A-treated *db/db* mice fasted overnight are similar to those of controls ( $n = 5$ ,  $P = \text{NS}$ ). **E:** The plasma GIP levels (pg/mL) in random-fed, anti-Nogo-A-treated *db/db* mice are similar to those of controls ( $n = 5$ ,  $P = \text{NS}$ ). **F:** Sensitivity of  $\beta$ -cells from isolated islets of control and 11C7-treated *db/db* mice in response to glucose supplemented with CC (10  $\mu\text{mol/L}$ ) or GLP-1 (100 nmol/L). Isolated islets from anti-Nogo-A-treated *db/db* mice secrete more insulin in response to 4.2 mmol/L + CC and higher glucose concentrations ( $n = 7-15$  batches of 10 islets, four mice,  $**P < 0.005$ ).

did not alter the fasting basal plasma PP level ( $n = 5$ ,  $P = \text{NS}$ ) (Fig. 5D). Similarly, like in Nogo-A KO mice, GIP levels were not affected by 2DG administration in random-fed anti-Nogo-A-treated *db/db* mice (Fig. 5E) ( $n = 5$ ,  $P = \text{NS}$ ). Altogether, these results suggest that the antibody-mediated neutralization of Nogo-A does not affect the vagal and incretin input on  $\beta$ -cells.

In parallel studies, anti-Nogo-A antibody was given to healthy control mice (C57BL/6J background). This treatment did not affect plasma levels of glucose or insulin (Supplementary Fig. 4), thus addressing a safety issue. The fact that 11C7 treatment has no effect on wild-type mice may be because they have normal parasympathetic input, contrary to Nogo-A KO and 11C7-treated *db/db* mice, which have a higher parasympathetic tone (Fig. 4A and Fig. 5D).

These observations were completed with the study of  $\beta$ -cell responsiveness to various secretagogues using isolated *db/db* islets cultured in the presence of glucose supplemented with 100  $\mu\text{mol/L}$  carbachol. Like the Nogo-A KO islets (above, Fig. 4B), islets from anti-Nogo-A-treated *db/db* mice displayed higher insulin secretion in the presence of glucose supplemented with carbachol ( $n = 7-15$ ,  $P < 0.05$ ), yet their sensitivity to glucose supplemented with GLP-1 was not affected (Fig. 5F).

Combined together, these different observations reveal that the administration of Nogo-A-neutralizing antibody enhances insulin secretion in diabetic *db/db* mice. Contrary to Nogo-A KO animals, the parasympathetic input on islets is not altered in anti-Nogo-A-treated *db/db* animals. However, as in Nogo-A KO mice,  $\beta$ -cell sensitivity to



glucose supplemented with carbachol is increased in *db/db* mice after Nogo-A downregulation.

Globally, the observations made with two independent experimental systems suggest that when Nogo-A activity is deleted or significantly impaired, the cholinergic vagal  $\beta$ -cell stimulation triggers a more potent release of insulin.  **$\beta$ -Cell replenishment after near-total  $\beta$ -cell loss is not improved by downregulation of Nogo-A.** Nogo-A is a negative modulator of regeneration in the CNS (23–25). We therefore explored if it has a similar function in regenerating an injured pancreas. We treated Nogo-A KO mice also bearing the *RIP-DTR* transgene with diphtheria toxin to induce the near-complete destruction of  $\beta$ -cells, as previously described (36). The trends in glycemia in these mice were followed for up to 3 months, reflecting the lack of any beneficial effect for the loss of Nogo-A (Supplementary Fig. 5A). Accordingly, the total pancreatic insulin content and  $\beta$ -cell mass were unaffected by the downregulation of Nogo-A, thus revealing that Nogo-A inactivation does not improve per se the regeneration capacity of the pancreas after extreme  $\beta$ -cell loss (Supplementary Fig. 5B and C), even though the genetic background of Nogo-A KO mice may somewhat influence the extent of recovery, as reported to occur for spinal cord regeneration (34).

## DISCUSSION

We report here that 1) Nogo-A is expressed in islet cells and that 2) its genetic inactivation results in increased insulin secretion through vagal stimulation due to a higher parasympathetic input and a higher responsiveness of  $\beta$ -cells to carbachol in the absence of Nogo-A. Similarly, 3) antibody-mediated neutralization of Nogo-A in diabetic *db/db* mice increases the vagal-induced insulin secretion, by increasing the sensitivity of  $\beta$ -cells to cholinergic stimuli. Finally, 4) contrary to what is observed in cells of the injured CNS, Nogo-A downregulation does not ameliorate the rate of  $\beta$ -cell regeneration in a model of total  $\beta$ -cell ablation.

The high vagal stimulation of insulin secretion was previously reported in obese patients (47,48) and in rodent models of T2D (*fa/fa* rats, preobese *ob/ob* mice, high fat-fed mice, and mice subjected to long-term glucose infusion or streptozotocin treatment) (49–54). Yet the precise involvement of the parasympathetic and sympathetic tones, and the sensitivity of  $\beta$ -cells, was not assessed in these studies. Using the high fat-fed model, Ahrén et al. (50) showed higher  $\beta$ -cell sensitivity to carbachol-induced insulin secretion in vitro.

**$\beta$ -Cell hypersensitivity in Nogo-A KO mice is independent of the glucose-stimulated insulin secretion pathway.** The molecular mode of action of Nogo-A in the pancreas is an intriguing question and deserves further study and elucidation. The changes at the parasympathetic-to- $\beta$ -cell synapse, possibly via the intracellular messengers of Nogo (Rho and  $\text{Ca}^{2+}$ ), as well as effects on pre- or postsynaptic cytoskeleton, are mechanisms that could be studied in dissociated coculture systems. Perhaps the signal transduction leading to insulin secretion is also altered; we found by quantitative PCR and deep sequencing on isolated islets that the relative  $\beta$ -cell expression of muscarinic and nicotinic receptors, which determine the sensitivity to cholinergic stimulation (55), as well as that of other cell signaling mediators, was identical in extracts from wild-type and Nogo-A KO isolated islets

(not shown). Interestingly, the expression of *Trpm2*, a  $\text{Ca}^{2+}$  channel, and serotonin receptor *Htr7*, well known to potentiate insulin secretion, was upregulated (46,56). We did not explore the activation of phospholipase C and the generation of IP<sub>3</sub> and diacylglycerol; however, we observed a similar secretory response to glucose or to glucose supplemented with KCl in isolated wild-type and Nogo-A KO islets (not shown). This suggests that, in the absence of Nogo-A, the improved insulin secretion in response to glucose/carbachol does not rely on the cell machinery involved in glucose/KCl-induced insulin secretion. Such dissociation in the sensitivity to different secretagogues was previously shown in other mutants, like those expressing a dominant-negative form of HNF1 $\alpha$  specifically in  $\beta$ -cells (38,50,57).

**Differential involvement of the parasympathetic input.** Insulin secretion is enhanced in diabetic *db/db* mice when Nogo-A activity is downregulated with antibody treatment; even though this effect is not mediated by a higher parasympathetic input to islets, it is nevertheless enhanced by it. However, the short exposure to anti-Nogo-A antibody (only two injections) was sufficient to increase the sensitivity of  $\beta$ -cells to glucose concentrations >4.2 mmol/L supplemented with carbachol. This observation alone raises new hopes in the quest for finding new ways to promote insulin secretion in diabetic patients.

The phenotype of 11C7-treated *db/db* mice partially recapitulates that of Nogo-A KO animals. It must be reiterated, though, that it is unclear whether intravenously injected monoclonal antibodies can cross the blood-brain barrier (58,59). In particular, it was shown that anti-Nogo-A antibody does not cross it (60); therefore, this would prevent any effect on the parasympathetic input from the CNS. However, we cannot completely exclude that a significant action of Nogo-A takes place outside the islets. Further exploration would be needed to fully address this aspect, such as by generating a  $\beta$ -cell-specific Nogo-A KO mouse. Yet, since Nogo-A downregulation also results in improved insulin secretion in vitro, from isolated islets, we conclude that Nogo-A acts locally (i.e., at the islet level). Together, these observations are compatible with Nogo-A action through combined mechanisms (intra- and extra-islet).

In conclusion, we have reported herein that Nogo-A is involved in glucose homeostasis. These results suggest that Nogo-A is a potential new target for antidiabetic drugs, by promoting insulin secretion in response to cholinergic stimuli, such as after food intake, without hypoglycemic events. We must recall, in this regard, that a neutralizing anti-human Nogo-A antibody is currently being tested in phase I clinical trials on acutely injured paraplegic patients in centers of the European Network of Spinal Cord Injury (M.E.S., in collaboration with Novartis). The inhibition of Nogo-A, for instance, with a weekly injection of antibody may thus represent an avenue for new antidiabetic treatments, by acting on the stimulatory input and thereby on insulin secretion from  $\beta$ -cells.

## ACKNOWLEDGMENTS

P.L.H. is the recipient of grants from the Juvenile Diabetes Research Foundation, the National Institutes of Health/National Institute of Diabetes and Digestive and Kidney Diseases (Beta Cell Biology Consortium), the Swiss National Science Foundation (member of the NCCR Frontiers in Genetics and the NRP63 Stem Cells and

Regenerative Medicine), and the European Union (IMIDIA consortium). P.H.L. is the recipient of grants from the Swiss National Science Foundation (Division III 310030-132705 and SPUM) and the Swiss Society for Multiple Sclerosis. C.B.B. and C.P. were recipients of grants from the Swiss National Science Foundation (FSBMB grants).

No potential conflicts of interest relevant to this article were reported.

C.B.B. conceived the experiments, performed all experiments and analyses, and wrote the manuscript. D.E.B. and C.P. conceived the experiments, performed all experiments and analyses, contributed to discussion, and reviewed the manuscript. M.B. performed all experiments and analyses. M.E.S. and P.H.L. contributed to discussion and reviewed the manuscript. P.L.H. conceived the experiments, analyzed the results, and wrote the manuscript. P.L.H. is the guarantor of this work and, as such, had full access to all the data in the study and takes responsibility for the integrity of the data and the accuracy of the data analysis.

The authors thank Claes B. Wollheim and Pierre Vassalli (University of Geneva Medical School) for their insightful comments. The authors also thank Berivan Polat for skillful technical help, Olivier Fazio for islet isolation, and Christian Vesin for the *in vivo* insulin secretion assays (University of Geneva Medical School). The authors thank Anis Mir (Novartis, Basel, Switzerland) for generously providing the anti-Nogo-A antibody (11C7), Frédéric Preitner and Marianne Carrard (University of Lausanne) for the Milliplex assay, Doug Melton (Harvard Medical School, Cambridge, MA) for sharing the *Pdx1-GFP* mice, Alexandre Dayer (University of Geneva Medical School) for the anti-GFAP antibody, Chris Wright for the anti-Pdx1 antibody, and Ole Madsen for the anti-PC1/3 antibody.

## REFERENCES

- Liu M, Hodish I, Haataja L, et al. Proinsulin misfolding and diabetes: mutant INS gene-induced diabetes of youth. *Trends Endocrinol Metab* 2010; 21:652–659
- D'Alessio DA, Kieffer TJ, Taborsky GJ Jr, Havel PJ. Activation of the parasympathetic nervous system is necessary for normal meal-induced insulin secretion in rhesus macaques. *J Clin Endocrinol Metab* 2001;86: 1253–1259
- Karlsson S, Åhrén B. CCK-8-stimulated insulin secretion *in vivo* is mediated by CCKA receptors. *Eur J Pharmacol* 1992;213:145–146
- Balkan B, Li X. Portal GLP-1 administration in rats augments the insulin response to glucose via neuronal mechanisms. *Am J Physiol Regul Integr Comp Physiol* 2000;279:R1449–R1454
- Thorens B. Physiology of GLP-1—lessons from glucocretin receptor knockout mice. *Horm Metab Res* 2004;36:766–770
- Straub SG, Sharp GW. Glucose-stimulated signaling pathways in biphasic insulin secretion. *Diabetes Metab Res Rev* 2002;18:451–463
- Teff KL. Visceral nerves: vagal and sympathetic innervation. *JPEN J Parenter Enteral Nutr* 2008;32:569–571
- Holst JJ, Grønholt R, Schaffalitzky de Muckadell OB, Fahrenkrug J. Nervous control of pancreatic endocrine secretion in pigs. II. The effect of pharmacological blocking agents on the response to vagal stimulation. *Acta Physiol Scand* 1981;111:9–14
- Campfield LA, Smith FJ. Neural control of insulin secretion: interaction of norepinephrine and acetylcholine. *Am J Physiol* 1983;244:R629–R634
- Ionescu E, Jeanrenaud B. Effect of electrical stimulation of the vagus nerve on insulinemia and glycemia in *Acomys cahirinus* mice. *Endocrinology* 1988;123:885–890
- Åhrén B, Taborsky GJ Jr. Effects of pancreatic noradrenaline infusion on basal and stimulated islet hormone secretion in the dog. *Acta Physiol Scand* 1988;132:143–150
- Karlsson S, Sundler F, Åhrén B. Neonatal capsaicin-treatment in mice: effects on pancreatic peptidergic nerves and 2-deoxy-D-glucose-induced insulin and glucagon secretion. *J Auton Nerv Syst* 1992;39:51–59
- Brunicaudi FC, Shaville DM, Andersen DK. Neural regulation of the endocrine pancreas. *Int J Pancreatol* 1995;18:177–195
- Teitelman G. Insulin cells of pancreas extend neurites but do not arise from the neuroectoderm. *Dev Biol* 1990;142:368–379
- Le Douarin NM. On the origin of pancreatic endocrine cells. *Cell* 1988;53: 169–171
- Suckow AT, Sweet IR, Van Yserloo B, et al. Identification and characterization of a novel isoform of the vesicular gamma-aminobutyric acid transporter with glucose-regulated expression in rat islets. *J Mol Endocrinol* 2006;36:187–199
- Baekkeskov S, Aanstoot HJ, Christgau S, et al. Identification of the 64K autoantigen in insulin-dependent diabetes as the GABA-synthesizing enzyme glutamic acid decarboxylase. *Nature* 1990;347:151–156
- Suckow AT, Comoletti D, Waldrop MA, et al. Expression of neurexin, neuroligin, and their cytoplasmic binding partners in the pancreatic beta-cells and the involvement of neuroligin in insulin secretion. *Endocrinology* 2008;149:6006–6017
- Suckow AT, Zhang C, Egodage S, et al. Transcellular neuroligin-2 interactions enhance insulin secretion and are integral to pancreatic beta-cell function. *J Biol Chem* 2012;287:16–26
- Chen MS, Huber AB, van der Haar ME, et al. Nogo-A is a myelin-associated neurite outgrowth inhibitor and an antigen for monoclonal antibody IN-1. *Nature* 2000;403:434–439
- Caroni P, Schwab ME. Antibody against myelin-associated inhibitor of neurite growth neutralizes nonpermissive substrate properties of CNS white matter. *Neuron* 1988;1:85–96
- Jokic N, Gonzalez de Aguilar JL, Pradat PF, et al. Nogo expression in muscle correlates with amyotrophic lateral sclerosis severity. *Ann Neurol* 2005;57:553–556
- Schwab ME. Nogo and axon regeneration. *Curr Opin Neurobiol* 2004;14: 118–124
- Cafferty WB, Strittmatter SM. The Nogo-Nogo receptor pathway limits a spectrum of adult CNS axonal growth. *J Neurosci* 2006;26:12242–12250
- Oertle T, van der Haar ME, Bandtlow CE, et al. Nogo-A inhibits neurite outgrowth and cell spreading with three discrete regions. *J Neurosci* 2003; 23:5393–5406
- Bareyre FM, Haudenschild B, Schwab ME. Long-lasting sprouting and gene expression changes induced by the monoclonal antibody IN-1 in the adult spinal cord. *J Neurosci* 2002;22:7097–7110
- Weiss J, Takizawa B, McGee A, et al. Neonatal hypoxia suppresses oligodendrocyte Nogo-A and increases axonal sprouting in a rodent model for human prematurity. *Exp Neurol* 2004;189:141–149
- Montani L, Gerrits B, Gehrig P, et al. Neuronal Nogo-A modulates growth cone motility via Rho-GTP/LIMK1/cofilin in the unlesioned adult nervous system. *J Biol Chem* 2009;284:10793–10807
- Grados-Munro EM, Fournier AE. Myelin-associated inhibitors of axon regeneration. *J Neurosci Res* 2003;74:479–485
- Aloy EM, Weinmann O, Pot C, et al. Synaptic destabilization by neuronal Nogo-A. *Brain Cell Biol* 2006;35:137–156
- Liu YY, Jin WL, Liu HL, Ju G. Electron microscopic localization of Nogo-A at the postsynaptic active zone of the rat. *Neurosci Lett* 2003;346:153–156
- Lee H, Raiker SJ, Venkatesh K, et al. Synaptic function for the Nogo-66 receptor NgR1: regulation of dendritic spine morphology and activity-dependent synaptic strength. *J Neurosci* 2008;28:2753–2765
- Simonen M, Pedersen V, Weinmann O, et al. Systemic deletion of the myelin-associated outgrowth inhibitor Nogo-A improves regenerative and plastic responses after spinal cord injury. *Neuron* 2003;38:201–211
- Dimou L, Schnell L, Montani L, et al. Nogo-A-deficient mice reveal strain-dependent differences in axonal regeneration. *J Neurosci* 2006;26:5591–5603
- Blum B, Hrvatin SS, Schuetz C, Bonal C, Rezanian A, Melton DA. Functional beta-cell maturation is marked by an increased glucose threshold and by expression of urocortin 3. *Nat Biotechnol* 2012;30:261–264
- Thorel F, Nepote V, Avril I, Kohno K, Desgraz R, Chera S, et al. Conversion of adult pancreatic alpha-cells to beta-cells after extreme beta-cell loss. *Nature* 2010;464:1149–1154
- Åhren B, Simonsson E, Scheurink AJ, Mulder H, Myrén U, Sundler F. Dissociated insulinotropic sensitivity to glucose and carbachol in high-fat diet-induced insulin resistance in C57BL/6J mice. *Metabolism* 1997;46:97–106
- Winzell MS, Pacini G, Wollheim CB, Åhren B. Beta-cell-targeted expression of a dominant-negative mutant of hepatocyte nuclear factor-1alpha in mice: diabetes model with beta-cell dysfunction partially rescued by nonglucose secretagogues. *Diabetes* 2004;53(Suppl. 3):S92–S96
- Persson-Sjögren S, Lindström P. Effects of cholinergic m-receptor agonists on insulin release in islets from obese and lean mice of different ages: the importance of bicarbonate. *Pancreas* 2004;29:e90–e99
- Rossi J, Santamäki P, Airaksinen MS, Herzig KH. Parasympathetic innervation and function of endocrine pancreas requires the glial cell line-derived factor family receptor alpha2 (GFRalpha2). *Diabetes* 2005;54: 1324–1330

41. Mansouri A, Aja S, Moran TH, et al. Intraperitoneal injections of low doses of C75 elicit a behaviorally specific and vagal afferent-independent inhibition of eating in rats. *Am J Physiol Regul Integr Comp Physiol* 2008;295: R799–R805
42. Karlsson S, Bood M, Åhrén B. The mechanism of 2-deoxy-glucose-induced insulin secretion in the mouse. *J Auton Pharmacol* 1987;7:135–144
43. Havel PJ, Taborsky GJ Jr. The contribution of the autonomic nervous system to changes of glucagon and insulin secretion during hypoglycemic stress. *Endocr Rev* 1989;10:332–350
44. Schwartz TW, Holst JJ, Fahrenkrug J, et al. Vagal, cholinergic regulation of pancreatic polypeptide secretion. *J Clin Invest* 1978;61:781–789
45. Althage MC, Ford EL, Wang S, Tso P, Polonsky KS, Wice BM. Targeted ablation of glucose-dependent insulinotropic polypeptide-producing cells in transgenic mice reduces obesity and insulin resistance induced by a high fat diet. *J Biol Chem* 2008;283:18365–18376
46. Togashi K, Hara Y, Tominaga T, et al. TRPM2 activation by cyclic ADP-ribose at body temperature is involved in insulin secretion. *EMBO J* 2006;25:1804–1815
47. Del Rio G, Procopio M, Bondi M, et al. Cholinergic enhancement by pyridostigmine increases the insulin response to glucose load in obese patients but not in normal subjects. *Int J Obes Relat Metab Disord* 1997;21:1111–1114
48. Tappy L, Chiolerio R, Randin JP, Burckhardt P, Felber JP. Effects of cholinergic stimulation and antagonism on plasma insulin concentration in lean and obese human subjects. *Horm Metab Res* 1986;18:821–826
49. Ostenson CG, Grill V. Evidence that hyperglycemia increases muscarinic binding in pancreatic islets of the rat. *Endocrinology* 1987;121:1705–1710
50. Åhrén B, Sauerberg P, Thomsen C. Increased insulin secretion and normalization of glucose tolerance by cholinergic agonism in high fat-fed mice. *Am J Physiol* 1999;277:E93–E102
51. Chen NG, Romsos DR. Enhanced sensitivity of pancreatic islets from preobese 2-week-old ob/ob mice to neurohormonal stimulation of insulin secretion. *Endocrinology* 1995;136:505–511
52. Balkan B, Dunning BE. Muscarinic stimulation maintains in vivo insulin secretion in response to glucose after prolonged hyperglycemia. *Am J Physiol* 1995;268:R475–R479
53. Laury MC, Takao F, Bailbe D, et al. Differential effects of prolonged hyperglycemia on in vivo and in vitro insulin secretion in rats. *Endocrinology* 1991;128:2526–2533
54. Rohner-Jeanrenaud F, Hochstrasser AC, Jeanrenaud B. Hyperinsulinemia of preobese and obese *fafa* rats is partly vagus nerve mediated. *Am J Physiol* 1983;244:E317–E322
55. Gilon P, Henquin JC. Mechanisms and physiological significance of the cholinergic control of pancreatic beta-cell function. *Endocr Rev* 2001;22: 565–604
56. Paulmann N, Grohmann M, Voigt JP, et al. Intracellular serotonin modulates insulin secretion from pancreatic beta-cells by protein serotonylation. *PLoS Biol* 2009;7:e1000229
57. Okabayashi Y, Otsuki M, Ohki A, Tani S, Baba S. Increased beta-cell secretory responsiveness to ceruletide and TPA in streptozocin-induced mildly diabetic rats. *Diabetes* 1989;38:1042–1047
58. Lampson LA. Monoclonal antibodies in neuro-oncology: getting past the blood-brain barrier. *MAbs* 2011;3:153–160
59. Pardridge WM. Molecular biology of the blood-brain barrier. *Mol Biotechnol* 2005;30:57–70
60. Merkler D, Oertle T, Buss A, et al. Rapid induction of autoantibodies against Nogo-A and MOG in the absence of an encephalitogenic T cell response: implication for immunotherapeutic approaches in neurological diseases. *FASEB J* 2003;17:2275–2277